# Shear viscosity of an ordering latex suspension

B. van der Vorst, D. van den Ende,* N. J. J. Aelmans, and J. Mellema
*J.M. Burgers Centre, Rheology Group, Faculty of Applied Physics, University of Twente, P.O. Box 217, 7500 AE Enschede, The Netherlands*
(Received 17 January 1997)

The shear viscosity of a latex which is ordered at rest is studied as a function of the shear rate and volume fraction. At low shear rates and for moderate to high volume fractions, the flow curves show dynamic yield behavior which disappears below a volume fraction of 8%. At high shear rates, the onset to the high shear rate plateau of the viscosity can be observed. A new model for the shear viscosity for lattices at high volume fractions is described. This model is based upon theories for the shear viscosity of dilute lattices of Blachford *et al.* [J. Phys. Chem. **73**, 1062 (1969)] and Russel [J. Fluid Mech. **85**, 673 (1978)]. In terms of this model, the ordered latex is broken down under shear flow into ordered domains suspended in a disordered fluid. The larger the shear rate, the smaller the volume fraction of ordered domains. The experimental results can be described reasonably well with the model discussed here. [S1063-651X(97)12808-2]

PACS number(s): 82.70.−y

## I. INTRODUCTION

The rheological behavior of charged colloidal particles dispersed in an electrolyte has been studied by many authors over the past two decades. The shear viscosity of these dispersions depends strongly on the volume fraction and the excess electrolyte concentration. For dilute dispersions, the influence of the excess electrolyte concentration on the low-shear limit of the viscosity has been studied intensively. In this respect, we can discriminate between three electroviscous effects which have been comprehensively treated by Russel [1–5] and Blachford *et al.* [6] among others. The primary effect is caused by the distortion of the diffuse double layer of ions surrounding each particle. The secondary effect is due to the electrostatic repulsion between the particles. The tertiary electroviscous effect, mentioned by Russel, is the influence of the intra-particle repulsions on the particle shape. Since the colloidal dispersions studied in this work consist of monodisperse charged polystyrene spheres dispersed in water, the latter effects is of no interest here. Consequently, only the primary and the secondary effect are left as electroviscous contributions to the viscosity. These theories have been compared to the viscosities measured by Stone-Masui and Watillon [7] and Chan *et al.* [8] for dilute suspensions.

The present paper studies the shear viscosity of a nondilute suspension with strongly interacting particles. Earlier experiments on this matter have been performed by Chen and Zukoski [9], Buscall [10], and Quemada [12]. Theoretical models have been given, e.g., by Buscall [10] and Quemada [12]. These models are based on a semiempirical expression for the viscosity of hard-sphere suspensions (e.g., Krieger-Dougherty formula) describing the volume fraction dependency of the shear viscosity. The volume fraction in this expression is replaced by an effective hard-sphere volume fraction which depends on the electrostatic interaction between the particles.

Here a first attempt is made to describe the shear viscosity for nondilute suspensions containing strongly interacting spheres by extrapolating the theories for dilute suspensions mentioned before to the high volume fraction regime. However, the microstructure of these suspensions in shear flow needs some extra consideration since for high volume fractions and sufficient low excess electrolyte concentrations the particles order into crystalline lattices at rest. In shear flow, the system can be seen as a quasihomogeneous ''blend'' formed by a solid phase coexisting with a fluid phase [11,12]. If the shear rate is increased the number of dislocations or the amount of the disordered phase increases at the expense of the ordered phase. How these ordered and disordered regions are organized is still an open question. Since it is impossible, due to multiple scattering, to perform light scattering experiments on polystyrene latices with high volume fractions ($\phi > 0.01$), we were unable to obtain results in this way on the microstructure of our own lattices. Other techniques like x-ray scattering or neutron scattering do not suffer from this problem but they are not easy to implement in a viscometer. In order to envisage the microstructure of sheared lattices, we can use scattering experiments performed by other investigators on similar systems in shear flow and numerical simulations performed on these dispersions. The experimental data as well as the numerical results do not reveal one picture of the microstructure of these systems in a shear flow. On the basis of light scattering experiments [11,13–15] and neutron scattering experiments [16], Ackerson and Clark [15] and Tomita and Van de Ven [11] concluded that the flow forces the particles to order in hexagonal plates which lie parallel to the shear plane and slide over each other. Experiments of Imhof *et al.* [17,18] and Dozier and Chaikin [19] show that the colloidal crystal breaks up into crystallites which are separated by disordered material. Here the crystallites gradually melt with increasing shear rate and eventually the suspension becomes completely disordered. Also numerical results of Stevens and Robbins [20] indicate a microstructure of solid crystal plates separated by disordered material where the shear is concentrated.

In this paper, we model our fluid as an ordered suspension

*Corresponding author.

 

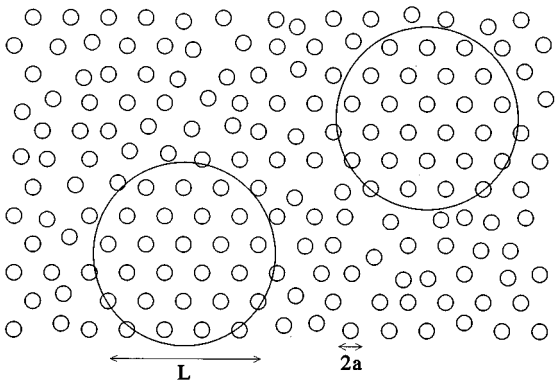


FIG. 1. The polystyrene latex modeled as a suspension of spherical aggregates of size $L$ (crystallites) in a fluid phase consisting of disordered particles of size $2a$.

which at rest consists of many crystallites separated by dislocations. If a shear is applied to this ordered suspension, the flow is most probably concentrated at the dislocation edges since the particles at these dislocations are more loosely trapped by the potential field of the particle interactions. This leads us to our working hypothesis that an at-rest ordering dispersion in shear flow can be considered as a suspension of crystallites or domains (aggregates) of ordered material dispersed in a disordered fluid phase (see Fig. 1). The consequences of this hypothesis on the shear rate dependence of the viscosity are investigated in terms of a microrheological model and compared with the experimental observations.

This paper is organized as follows: In Sec. II the model for the viscosity of a nondilute colloidal dispersion consisting of strongly interacting particles is described. In Sec. III, the dispersion and setup of the experiments are shortly described. Finally, in Sec. IV the experimental and theoretical results are discussed.

## II. THEORY

Under shear we consider the fluid as a suspension which consists of disordered material in which the crystallites or aggregates of ordered material are suspended (see Fig. 1). Increasing the shear rate causes the aggregates to become smaller in favor of the disordered material that separates the crystallites. The flow is concentrated in the disordered or fluidlike phase if the penetration depth of the flow field into the ordered aggregates is small compared to the size $L$ of the aggregates. According to Wiegel [21] the penetration depth of the flow field into an aggregate is maximal $d_{\max}=\sqrt{\eta_0/(\zeta_0 C)}$. Here $\eta_0$ is the viscosity of the solvent, $\zeta_0$ is Stokes' friction coefficient $6\pi\eta_0 a$ for a free particle, and $C=3\phi/(4\pi a^3)$ is the particle number concentration; $a$ is the radius of a particle. In our case the maximal penetration depth of the flow field into the aggregates is approximately 100 nm which is more than five times smaller than the interparticle distance in the lattice so the aggregates are considered as impenetrable.

Conceiving the aggregates as hard spheres, the total shear viscosity of the suspension $\eta(\dot\gamma)$ can be modeled with the Krieger-Dougherty expression

$$\eta=\eta_{\rm fl}(\dot\gamma)\left(1-\frac{\phi_{\rm cr}(\dot\gamma)}{\phi_{\rm cr}^{\max}}\right)^{-2.5\phi_{\rm cr}^{\max}} \tag{1}$$

in which both the volume fraction of crystalline aggregates $\phi_{\rm cr}$ and the shear viscosity of the disordered phase $\eta_{\rm fl}$ depend on the shear rate $\dot\gamma$ applied to the suspension. These two quantities will be considered in the next sections.

### A. Viscosity of the disordered phase

For a dilute latex the electrostatic force is dominated by the Brownian force and no ordering will occur; also the low-shear viscosity will be dominated by Brownian interactions. For a nondilute latex at rest the maximum separation ($\approx 2a\phi^{1/3}$) of the particles is so small that the Brownian force on the particles is dominated by the electrostatic force causing the particles to order in a crystal. In flow, these ordered structures are broken down by hydrodynamic interactions. Consequently in our investigations only the hydrodynamic and electrostatic forces have been taken into account.

The shear viscosity of the disordered phase is calculated from the electrostatic shear stress following Blachford *et al.* [6] and Russel [2]. We start from the force balance on one particle, omitting inertial effects since the time scale on which these are important is much smaller than the diffusive time scale on which the equation is valid. The total electrostatic force on a particle can be reduced to a summation of the electrostatic pair interactions with its nearest neighbors because the Debye screening length $\kappa^{-1}$ is smaller than one-third of the surface to surface distance between two particles in our latex dispersions [22].

The electrostatic stress in the suspension can be calculated by considering a ''collision'' between two particles $i$ and $k$ in the suspension surrounded by many other particles. If the two particles are separated by one or more other particles, the electrostatic interaction, $\vec F_{ik}^{\,I}$, between the two particles is screened and it is sufficient to take into account only electrostatic interactions between nearest neighbors [22]. If, however, the distance between the two particles, $\vec r_{ik}$, becomes on the order of the interparticle distance $R_{\rm eq}$, which is approximately $2a\phi^{-1/3}$, or less, they do interact, which will contribute to the stress in the suspension. Averaging $\vec F_{ik}^{\,I}\vec r_{ik}$ along the collision path and over all possible initial configurations results in the electrostatic contribution to the stress in the suspension. To calculate the trajectory of particle $i$ when it collides with particle $k$ the total electrostatic force $\vec F_i^{\,I}$ on particle $i$ is modeled as the sum of the force $\vec F_{ik}^{\,I}(\vec r_{ik})$ due to particle $k$ and an average contribution $F_a\hat r_{ik}$ from the other nearest neighbor particles

$$\vec F_i^{\,I}=[F_{ik}^{I}(\vec r_{ik})-F_a]\hat r_{ik} \tag{2}$$

with $\hat r_{ik}=\vec r_{ik}/r_{ik}$. $F_a$ is determined from the equilibrium condition at rest

$$F_a = \sum_{j=1, j\neq i, j\neq k}^{N_n} |\vec{F}_{ij}^{I}(\vec{r}_{ij}^{\,\mathrm{eq}})| = |\vec{F}_{ik}^{I}(\vec{r}_{ik}^{\,\mathrm{eq}})| \tag{3}$$

with $\vec{r}_{ik}^{\,\mathrm{eq}} = |\vec{r}_i^{\,\mathrm{eq}} - \vec{r}_k^{\,\mathrm{eq}}|$. $N_n$ is the number of nearest neighbors and $\vec{F}_{ij}^{I}$ is the electrostatic force on particle $i$ due to particle $j$. In a steady shear flow the force balance for particle $i$ during a collision with particle $k$ is under these assumptions given by

$$\vec{F}_i^H + \vec{F}_i^I = \vec{O}, \tag{4}$$

where $\vec{O}$ is the zero vector. The hydrodynamic force $\vec{F}_i^H$ on particle $i$ is given by

$$\vec{F}_i^H = \zeta(\vec{v}_{\mathrm{fl}} - \vec{v}_i), \tag{5}$$

where $\vec{v}_i = d\vec{r}_i/dt$ is the velocity of the particle, $\vec{v}_{\mathrm{fl}}$ the fluid velocity at $\vec{r}_i$, and $\zeta$ is the volume-fraction dependent friction factor of the particles. The friction factor is modeled by

$$\zeta = 6\pi\eta(\phi)a + f\frac{2\pi\Phi_a^2 a\epsilon_r\epsilon_o}{3D_i}\kappa a(1+\kappa a)^2. \tag{6}$$

The first term is due to the hydrodynamic friction of the latex particle in a dispersion of hard spheres. The viscosity in this expression is calculated from the Krieger-Dougherty equation: $\eta(\phi) = \eta_o(1-\phi/\phi_m)^{-2.5\phi_m}$. When a latex particle moves through its solvent, the layer of counterions exerts an additional drag force on the particle. This electrodynamic friction is taken into account by the second term in Eq. (6). This term is the low frequency limit of the electrodynamic friction coefficient $\zeta_e(\omega)$ as derived by Felderhof and Jones [23]. $\Phi_a$ is the apparent surface potential and $\kappa$ is the effective reciprocal Debye length. Both can be calculated from the cell model described by Van der Vorst *et al.* [22]; $\epsilon_r\epsilon_o$ is the dielectric constant of the fluid. The only counterions in our model fluid are $H^+$ ions which have a diffusion constant $D_i = 9.5\times10^{-9}\ \mathrm{m^2\ s^{-1}}$ and a valence $z=1$. The factor $f$ is a fit parameter of our model. It is an unknown parameter on the order of unity with which deviations might be corrected stemming from deformations of the spherical double layer or pollution with less mobile ions ($Na^+$ or $K^+$). The electrostatic force between the two particles is modeled with the expression used by Van der Vorst *et al.* [22] to describe the static shear modulus

$$\vec{F}_{ik}^{I}(\vec{r}) = 4\pi\epsilon_r\epsilon_o\Phi_a^2(\kappa a)^2 e^{2\kappa a}\frac{2\kappa r+1}{(2\kappa r)^2}e^{-2\kappa r}\vec{e}_r \tag{7}$$

with $2r$ the center to center distance between the two particles. Substitution of Eqs. (5) and (7) in Eq. (4) leads to the following trajectory equation:

$$\frac{dY}{d\xi} = Y\frac{\xi}{1+\xi^2} + \frac{H}{\sin\phi_0}\left(\frac{Y+1}{Y^2}e^{-Y} - \frac{Y_0+1}{Y_0^2}e^{-Y_0}\right) \tag{8}$$

with $Y = 2\kappa r$ the dimensionless distance of the particle to the center of the cell, $Y_0 = \kappa R_{\mathrm{eq}}$ the equilibrium distance, $H = [4\pi\epsilon_r\epsilon_0\Phi_a^2(\kappa a)^2 e^{2\kappa a}2\kappa]/(\zeta\dot{\gamma})$ and $\xi = \cot\theta$. $H$ times the term in brackets represents the ratio between the electrostatic interaction force between the two particles and the hydrodynamic force upon the particles. A spherical coordinate system has been used in which the origin coincides with the center of mass of the two particles (see Fig. 2). The flow direction is along the $z$ axis while the gradient is directed along the $y$ axis. This approach is similar to that of Blachford *et al.* [6] except for a little difference in the coordinate system. The trajectories of both particles can be calculated by numerical integration of Eq. (8) using a Runge-Kutta integration scheme.

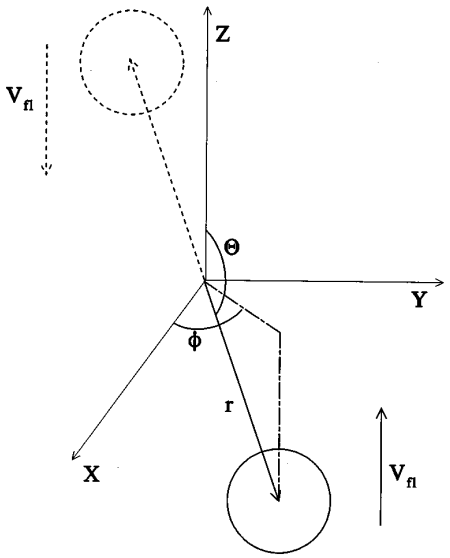


FIG. 2. The collision between two charged polystyrene latex particles in a shear flow.

We are interested in the (shear) stress component $T_{yz}$ generated by all the colliding pairs. The contribution of the electrostatic interaction to this stress component can be calculated with [24]

$$T_{yz}(t) = \int\int\int (q_y F_z^I)\Phi(\vec{q},t;\vec{p},\tau)\ d^3p\ d^3q\ d\tau. \tag{9}$$

$\Phi(\vec{q},t;\vec{p},\tau)\ d^3p\ d^3q\ d\tau$ is defined as the number density of pairs at time $t$ with a connection vector in $d^3q$ around $\vec{q}$ which were created between $t-\tau-d\tau$ and $t-\tau$ with a connection vector in $d^3p$ around $\vec{p}$. Assuming a steady state situation, the only time dependence is the lifetime of a connection. The distribution $\Phi$ can be written as a product of three contributions

$$\Phi(\vec{q},t;\vec{p},\tau)\ d^3p\ d^3q\ d\tau = \{\dot{n}_{\mathrm{cr}}\ d^3p\ d\tau\}\{P_{\mathrm{surv}}(\vec{p},\tau)\} \times\{P_{\mathrm{trans}}(\vec{q};\vec{p},\tau)\ d^3q\}. \tag{10}$$

$\dot{n}_{\mathrm{cr}}\ d^3p\ d\tau$ is the number density of pairs created in a volume $d^3p$ around $\vec{p}$ within a period $d\tau$. $P_{\mathrm{surv}}(\vec{p},\tau)$ is the survival probability of a pair created at $\vec{p}$ after a period $\tau$ and $P_{\mathrm{trans}}(\vec{q};\vec{p},\tau)$ is the probability that a pair created in $d^3p$ around $\vec{p}$ translates to $d^3q$ around $\vec{q}$ during a period of time $\tau$, given it still exists. The number of created connections is

determined by the number of particles flowing into a sphere with radius $R_{eq}$ around the central particle:

$$\dot{n}_{cr}\ d^3p\ d\tau = \delta(p-R_{eq})\frac{1}{2}n^2\dot{\gamma}p^3\sin\phi_0\cos\theta_0 \times \sin^2\theta_0\ dp\ d\theta_0\ d\phi_0\ d\tau. \quad (11)$$

Here $d^3p$ is written as $p^2\sin\theta_0\, d\theta_0\, d\phi_0\, dp$, $n$ is the number density of particles, and $\delta$ is the Dirac function. Because the Brownian motion of the particles is omitted the trajectories of the colliding particles are fully deterministic. By defining $\vec{r}(\vec{p},\tau)$ as the pair vector which has been created at $\vec{p}$ a time $\tau$ before, the translation probability can be written as

$$P_{trans}(\vec{q};\vec{p},\tau) = \delta(\vec{q}-2\vec{r}(\vec{p},\tau)). \quad (12)$$

The survival probability can be written as

$$P_{surv}(\vec{p},\tau) = \begin{cases} 1 & \text{if } \tau < \tau_{\not\prec}(\vec{p}), \\ 0 & \text{if } \tau > \tau_{\not\prec}(\vec{p}), \end{cases} \quad (13)$$

where $\tau_{\not\prec}(\vec{p})$ is the time elapsed when a pair which was created with connection vector $\vec{p}$ is broken up. In this case $\tau_{\not\prec}$ is the time the interacting pair remains within a distance $R_{eq}$ from each other. By substitution of Eqs. (11)–(13), and (10) into (9) and carrying out the integration over the $\vec{q}$ space and over $p$ one deduces

$$T_{yz} = \frac{A}{2\kappa}n^2\dot{\gamma}(R_{eq})^3\int_0^{\pi}d\phi_0\int_{-\infty}^{0}d\xi_0\int_{\xi_0}^{\xi_m}d\xi \times\left(\frac{1+Y}{Y}e^{-Y}\frac{\xi}{1+\xi^2}\right)\left(\frac{\xi_0}{1+\xi_0^2}\right)(1+\xi_0^2)^{5/2}\sin\phi_0 \quad (14)$$

with $\xi_0=\cot\theta_0$, $\xi_m=\cot\theta_m$, and $A=4\pi\epsilon_r\epsilon_0\Phi_a^2(\kappa a)^2e^{2\kappa a}$. The particle pair is created under an angle $\theta_0$ at time $\tau=0$ on the cell surface $Y=\kappa R_{eq}$. After a time $\tau_{\not\prec}$ the pair breaks up at $\theta_m$ with $Y=\kappa R_{eq}$ again. The trajectory of the particle in this equation $Y(\xi,\phi_0)$, $\xi(\xi_0,\phi_0,\dot{\gamma}\tau)$ is calculated from Eq. (8).

### B. The volume fraction of the ordered phase

In the proposed model, the ordered phase consists of spherical crystallites of size $L$ that occupy a fraction $\phi_{cr}$ of the total volume. The size and volume fraction are determined by breakup and coalescence processes.

The breakup of crystallites is described with a criterion obtained from fracture mechanics. It states that a deformed crystal will break up when the elastic energy stored in the deformed crystallite exceeds the energy needed to create a new free surface in the crystallite [25]:

$$\frac{\Sigma^2}{2G_0}V \geqslant E_sS. \quad (15)$$

Here $\Sigma$ is the shear stress in the crystal, $G_0$ is the shear modulus of the crystal, $V$ is the volume of a crystallite, $E_s$ is the breakup energy per unit area needed to create a free surface in the crystallite, and $S$ is the created free surface. In this expression, it is not directly clear how $E_s$ depends on the crystal properties. However, an expression for this energy can be found by identifying the energy needed to create a free surface in a crystallite with the energy needed to excite all the particles in this surface from their lattice sites to an unbounded state. The energy to excite one particle can be found from the melting criterion of Lindemann [26], which states that if $\langle d^2\rangle \geqslant \alpha^2R_{cr}^2$, where $\langle d^2\rangle$ is the mean-squared displacement of a particle from its lattice position, $\alpha$ is the Lindemann factor and $R_{cr}$ is the lattice parameter, the particle can no longer be considered as bounded to a lattice site. The minimum energy needed to excite one particle to this unbounded state is equal to $\frac{1}{2}k\alpha^2R_{cr}^2$, where $k=\nabla^2\Psi$ with $\Psi$ the total interaction energy of the particle. In our case, this melting energy is realized by both the Brownian energy $(3k_BT/2)$ and the energy due to the shearing of the crystal. In this respect, the minimum energy which the shear flow has to provide in order to excite one particle to the unbounded state divided by the specific shear surface of one particle $(\approx\pi R_{cr}^2)$ becomes

$$E_s \equiv \frac{k(\alpha^2R_{cr}^2-d_0^2)}{2\pi R_{cr}^2} \quad (16)$$

with $kd_0^2 \equiv 3k_BT$. By substitution of Eq. (16) in Eq. (15) with $V\approx L^3$ and $S\approx L^2$, the following breakup criterion can be derived for a crystallite: no breakup occurs as long as

$$\frac{\Sigma^2}{2G_0}L \leqslant \frac{k(\alpha^2R_{cr}^2-d_0^2)}{2\pi R_{cr}^2}. \quad (17)$$

In this way, the upperbound size of the crystallites in a shear flow is determined. The lower bound on $L$ can be derived from the coalescence of crystallites which is induced by the shear flow. An expression for the minimum size of the crystallites below which they do not coalesce is derived by comparing the shear force and the lubrication force on two colliding aggregates

$$\frac{6\pi\eta L^2\dot{\gamma}}{4} \leqslant \frac{6\pi\eta_{fl}L^3\dot{\gamma}}{16h}, \quad (18)$$

where the left-hand side of the equation represents the shear force on a spherical crystallite colliding with another sphere of size $L$, and the right-hand side represents the repulsive lubrication force along the connecting vector between two crystallites with radius $L/2$ that approach each other with a velocity $L\dot{\gamma}$ [5]. The velocity difference between the disordered phase and a stationary aggregate is estimated as $L\dot{\gamma}/2$; $\eta$ is the shear viscosity of the total suspension, $\eta_{fl}$ is the viscosity of the disordered phase between the aggregates and $h$ is the surface to surface distance between the two aggregates. The minimum distance $h_{min}$ is determined from Eq. (18). If this distance is smaller than the average separation distance between the particles, all of the disordered phase is squeezed out of the gap, the surfaces of the two aggregates make contact and the two crystallites coalesce.

The shear melting criterion (17) together with the shear coalescence criterion (18) determines the range of sizes for which the aggregates are stable at a certain aggregate volume fraction,

$$\frac{4\eta R_{\mathrm{cr}}}{\eta_{\mathrm{fl}}} \leqslant L \leqslant \frac{2G_0}{\Sigma^2}\frac{k(\alpha^2 R_{\mathrm{cr}}^2 - d_0^2)}{2\pi R_{\mathrm{cr}}^2}. \tag{19}$$

### C. Numerical implementation

Since the viscosity of the fluid phase is shear rate dependent, the average shear rate in the fluid phase has to be known. It can be calculated from the observation that the energy dissipation in the total suspension equals that in the fluid phase since no energy is dissipated in the hard-sphere aggregates:

$$\dot{\gamma}_{\mathrm{fl}} = \dot{\gamma}\sqrt{\frac{\eta}{\eta_{\mathrm{fl}}}\frac{V_{\mathrm{tot}}}{V_{\mathrm{fl}}}} = \dot{\gamma}\left(1-\frac{\phi_{\mathrm{cr}}}{\phi_{\mathrm{cr}}^{\max}}\right)^{-(5/4)\phi_{\mathrm{cr}}^{\max}}(1-\phi_{\mathrm{cr}})^{-1/2}. \tag{20}$$

Here $V_{\mathrm{tot}}$ is the suspension volume and $V_{\mathrm{fl}}$ is the volume occupied by the fluid phase. The last step is performed by substitution of Eq. (1). In the stationary case the breakup process is equilibrated by the coalescence of crystallites. We assume that the suspension adopts the maximum volume fraction of aggregates and the inequality signs in Eq. (19) have been replaced by equality signs. This results in a second expression for $\eta(\dot{\gamma},\phi)$

$$\frac{4\eta R_{\mathrm{cr}}}{\eta_{\mathrm{fl}}} = \frac{2G_0}{(\eta\dot{\gamma})^2}\frac{k(\alpha^2 R_{\mathrm{cr}}^2 - d_0^2)}{2\pi R_{\mathrm{cr}}^2}, \tag{21}$$

where $\eta\dot{\gamma}$ is substituted for the shear stress $\sigma$ on the aggregates. From Eqs. (1), (14), (20), and (21) the suspension viscosity is calculated using a numerical scheme given in Fig. 3.

Besides $\dot{\gamma}$, $\phi$, the particle radius $a$ and the surface charge density $\sigma$ the viscosity model contains the parameters $\phi_{\mathrm{cr}}^{\max}$, $k$, $G_0$, $d_0$, $R_{\mathrm{cr}}$, $R_{\mathrm{eq}}$, $f$, $\phi_m$, $\alpha$, and $n_b$. The maximum packing fraction of crystallites $\phi_{\mathrm{cr}}^{\max}$ in Eq. (1) is chosen equal to 0.71. This is the maximum packing fraction derived from experiments on the shear viscosity of hard-sphere suspensions at high shear rates [27,5]. The distance $R_{\mathrm{cr}}$ is chosen equal to $0.904\times 2a\phi^{-1/3}$, which is the distance in a fcc lattice. The values for $k$ and $G_0$, which are both functions of ($\phi$, $a$, $\sigma$, and $n_b$), are obtained from calculations described by Van der Vorst *et al.* [22] and $d_0^2 = 3k_BT/k$. The Lindemann factor $\alpha$ is estimated to be 0.2 which is close to the range of experimental and theoretical results found for this factor [28,29]. Besides by $G_0$ the viscosity of the fluid phase is determined by three parameters: $R_{\mathrm{eq}}$, $f$, and $\phi_m$. Since the Peclet number for the latex particles is smaller than one for the majority of shear rates (i.e., all shear rates smaller than approximately 20 $\mathrm{s}^{-1}$), $\phi_m$ is chosen equal to 0.63 [27,5]. The distance $R_{\mathrm{eq}}$ is chosen equal to $0.974\times 2a\phi^{-1/3}$. The last two parameters $f$ and $n_b$ are unknown and have been used as fitting parameters.

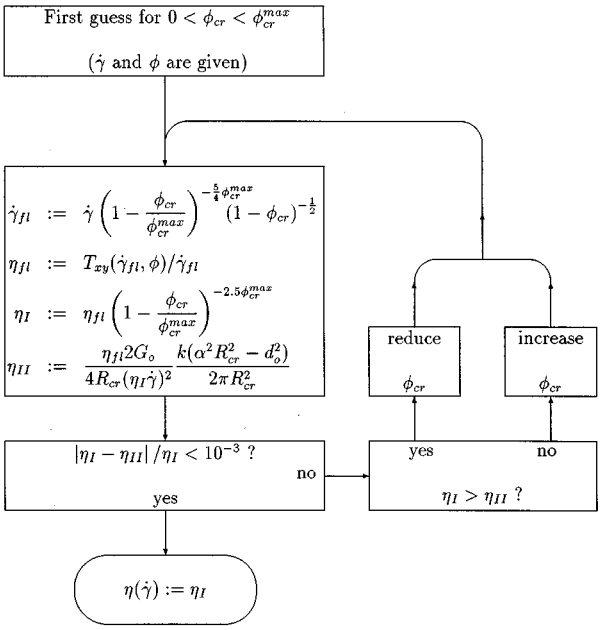


FIG. 3. Calculation scheme of $\eta(\dot{\gamma})$.

## III. EXPERIMENTAL

In the experimental part of this investigation, we used a monodisperse polystyrene latex which has been synthesized following the method described by Goodwin *et al.* [30]. A comprehensive treatment of the synthesis of lattices has been given by Hearn *et al.* [31]. The purification and characterization of the samples have been described in detail by Van der Vorst *et al.* [22]. Two batches of polystyrene latex have been used with the following characteristics: For latex I the particle radius is 240 nm and the surface charge density is $-5.7\ \mu\mathrm{C/cm}^2$; for latex II the particle radius is 195 nm and the surface charge density is $-4.6\ \mu\mathrm{C/cm}^2$. The electrolyte concentration of the latex dispersions used in our experiments has been reduced with an ion-exchange resin (no excess electrolyte was added to the dispersions after this reduction) and the electrolyte concentration is estimated to be 10 $\mu$M [22]. The volume fractions of the studied latex dispersions vary between 0.05 and 0.35.

The viscometric measurements on polystyrene lattices have been performed on a Contraves LS 40 rheometer with a concentric cylinder geometry, a vapor lock, and a guard ring. For the geometry used the shear rate can be varied between 0.001 and 100 $\mathrm{s}^{-1}$ and shear stresses can be measured within the range of 0.001 to 5 Pa.

## IV. RESULTS AND DISCUSSION

The measurements shown in Figs. 4 and 5 are averaged over at least three flow curves. These curves reproduced within 50%. The error bars shown in Fig. 4 for a volume fraction of 0.155 are representative for the errors in the viscosity measured for the other volume fractions. In these figures, also the flow curves predicted by the model are shown. In both cases they result from one simultaneous fit of the model to the experimental data at the different volume fractions. The experimental data in Figs. 4 and 5 show the characteristic behavior of the lattices. At low shear rates and for

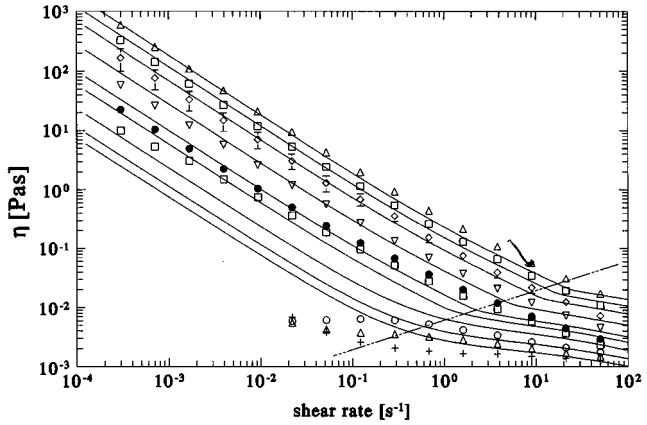


FIG. 4. The shear stress of latex I ($a=240$ nm, $\sigma=-5.7$ $\mu$C/cm$^2$) measured as a function of the shear rate for several volume fractions. The model results indicated by the solid lines are calculated for a electrolyte concentration 12 $\mu$M and $f=0.8$. Volume fractions: (+) 0.05, (△) 0.06, (○) 0.075, (□) 0.09, (●) 0.10, (▽) 0.125, (◇) 0.155, (□) 0.178, (△) 0.20. The dashed line indicates the transitions to completely disordered fluid.

volume fractions above 8% the viscosity is almost inversely proportional to $\dot{\gamma}$, i.e., the shear stress becomes almost independent from the shear rate. This behavior has also been observed by Chen *et al.* [32] who defined the constant stress found at low shear rates as the ''dynamic yield stress.'' Below a certain volume fraction the dynamic yield stress disappears and the experiments suggest a low shear viscosity plateau ($\eta_0$). At high shear rates and high volume fractions the onset to a high shear viscosity plateau ($\eta_\infty$) can be seen. The experimental values for the dynamic yield stress $\tau_0^{\rm dyn}=\lim_{\dot{\gamma}\to 0}[\dot{\gamma}\eta(\dot{\gamma})]$ can be determined from the curves shown in Figs. 4 and 5. For latex II also the static shear modulus $G_0$ has been measured by Van der Vorst *et al.* [22]. In Fig. 6, the dynamic yield stress has been plotted versus the

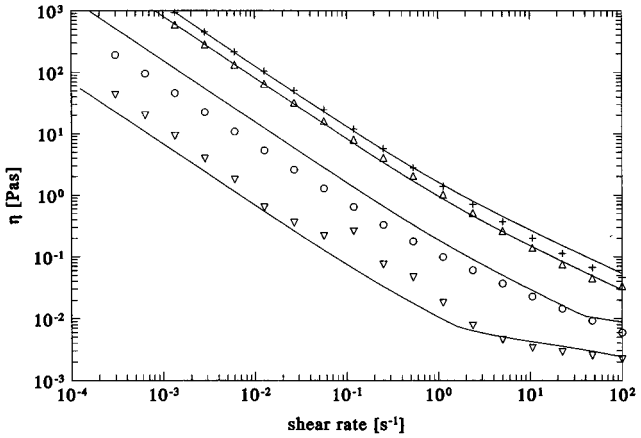


FIG. 5. The shear stress of latex II ($a=195$ nm, $\sigma=-4.6$ $\mu$C/cm$^2$) measured as a function of the shear rate for several volume fractions. The model results indicated by the solid lines are calculated for a electrolyte concentration 25 $\mu$M and $f=0.4$. Volume fractions: (▽) 0.10, (○) 0.19, (△) 0.30, (□) 0.35.

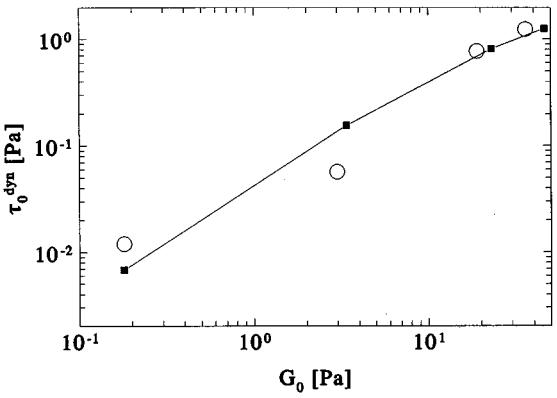


FIG. 6. The measured dynamic yield stress (obtained from Fig. 5) is plotted vs the measured elastic modulus. The model calculations are shown as solid symbols connected by a solid line.

static shear modulus. In addition, the curve resulting from our model calculations is shown in this figure.

Comparing the experimental results to the theoretical predictions for latex I in Fig. 4, one observes that the experiments at high volume fractions ($\phi=0.155$, 0.178, and 0.20) are described rather well by the first-order model presented here. At volume fractions below the phase transition ($\phi=0.05$, 0.06, and 0.075) the experiments show no yield behavior while our model still predicts a dynamic yield stress. This discrepancy is due to the fact that Brownian motion is not taken into account in the model for the viscosity of the fluid phase although in this regime of $\phi$ the electrostatic repulsion no longer dominates the Brownian interactions (see Sec. II A). At volume fractions above the phase transition, the calculated transition from yield behavior to high shear viscosity is sharper than observed in the experiments. This rather sharp edge in the model curves for moderate and high volume fractions indicates the point at which the solid phase melts away (see Fig. 7). This means that for shear rates above this transition (i.e., below the dashed line

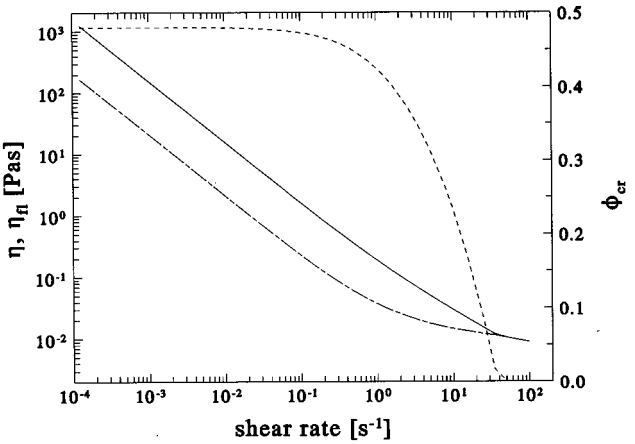


FIG. 7. The suspension viscosity ($\eta$, solid line), the viscosity of the fluid phase ($\eta_{\rm fl}$, dash-dotted line), and the aggregate volume fraction ($\phi_{\rm cr}$, dashed line) are plotted as a function of the shear rate. The calculation has been performed for latex II with $\phi=0.19$.

in Fig. 4) the viscosity is essentially the viscosity of the disordered fluid which is quite well described by our model, while for shear rates below this transition (i.e., above the dashed line in Fig. 4) the viscosity and yield behavior are mainly determined by the volume fraction of aggregates $\phi_{cr}$. For $\phi > 0.1$ the yield behavior predicted by the model agrees with the experimental observations. Comparing the experimental data with the model curves, one observes that, in our model, the solid phase melts down too strongly as a function of the shear rate for $\phi > 0.08$.

In Fig. 5 one observes more or less the same behavior for a latex II. Now only volume fractions above the phase transition were used and all curves indicate the yield behavior at low-shear rates. The predicted stress for the volume fractions 0.10, 0.30, and 0.35 describes the experimental results rather well. However, the calculated values for $\phi = 0.19$ are larger than the experimental ones. We have fitted the model simultaneously to all curves by adjusting the electrolyte concentration to 25 $\mu$M. The flow curve, especially the dynamic yield stress, depends rather strongly on the electrolyte concentration and a small increase of the electrolyte concentration to 30 $\mu$M reduces the dynamic yield stress at $\phi = 0.19$ by a factor 1.5. So a small pollution of the sample can be responsible for deviations like this one.

One expects the dynamic yield stress to scale linear with the static shear modulus [33,9]. The value predicted by Buscall [33] for this quantity is on the order of magnitude of 0.01 while Chen and Zukoski [9] derived 0.04.The slope $\beta$ obtained from the linear fit $\tau_0^{dyn} = \beta G_0$ to our measurements is $0.035 \pm 0.005$. This value is in keeping with the ratios found by Chen and Zukoski [9] and Chow and Zukoski [34] who found $\beta = 0.035 \pm 0.005$ and $0.029 \pm 0.006$, respectively. In addition, it is observed in Fig. 6 that the scaling behavior is descibed rather well by our model, although in our model $\beta$ slightly depends on $G_0$.

The sensitivity of the calculated flow curves on variations in the other parameters has also been investigated. This led us to conclude that our model mainly is sensitive for four parameters: the excess electrolyte concentration $n_b$, the Lindemann factor $\alpha$, and the radius $R_{eq}$ for which the yield behavior is sensitive: $\Delta\tau_0^{dyn}/\tau_0^{dyn} = 3\Delta\alpha/\alpha$ and $\Delta\tau_0^{dyn}/\tau_0^{dyn} = 5\Delta R_{eq}/R_{eq}$, respectively, and the factor $f$ for which the high shear viscosity is sensitive: $\Delta\eta_\infty/\eta_\infty = 2.5\Delta f/f$.

Although this is a first attempt to model the shear viscosity of a nondilute dispersion of strongly interacting particles, the model proposed describes the main behavior of the measured viscosity as a function of $\dot{\gamma}$ quite well for volume fractions above the phase transition where the influence of the Brownian motion is dominated by the repulsion between the particles. For these volume fractions the observed dynamic yield behavior can be understood from the volume fraction of ordered domains, while at higher shear rates the ordered domains are broken down and the measured viscosity is that of the disordered fluid phase, which is also rather well described by the model. These conclusions support our working hypothesis that an at rest ordering dispersion in shear flow can be considered as a suspension of crystallites (i.e., domains of ordered material) dispersed in a disordered fluid phase.


[1] W.B. Russel, J. Colloid Interface Sci. **55**, 590 (1976).
[2] W.B. Russel, J. Fluid Mech. **85**, 209 (1978).
[3] W.B. Russel, J. Fluid Mech. **85**, 673 (1978).
[4] W.B. Russel, J. Fluid Mech. **92**, 401 (1979).
[5] W.B. Russel, D.A. Saville, and W.R. Schowalter, *Colloidal Dispersions* (Cambridge University Press, Cambridge, England, 1989).
[6] J. Blachford, F.S. Chan, and D.A.I. Goring, J. Phys. Chem. **73**, 1062 (1969).
[7] J. Stone-Masui and A. Watillon, J. Colloid Interface Sci. **28**, 187 (1968).
[8] F.S. Chan, J. Blachford, and D.A.I. Goring, J. Colloid Interface Sci. **22**, 378 (1966).
[9] L.B. Chen and C.F. Zukoski, J. Chem. Soc. Faraday Trans. **86**, 2629 (1990).
[10] R. Buscall, J. Chem. Soc. Faraday Trans. **87**, 1365 (1991).
[11] M. Tomita and T.G.M. van de Ven, J. Colloid Interface Sci. **99**, 374 (1984).
[12] D. Quemada, Europhys. Lett. **25**, 149 (1994).
[13] B.J. Ackerson and N.A. Clark, Phys. Rev. A **30**, 906 (1984).
[14] B.J. Ackerson and P.N. Pusey, Phys. Rev. Lett. **61**, 1033 (1988).
[15] R. H. Ottewill and A.R. Rennie, Int. J. Multiphase Flow **16**, 681 (1986).
[16] B.J. Ackerson, J.B. Hayter, N.A. Clark, and L. Cotter, J. Chem. Phys. **84**, 2344 (1986).
[17] A. Imhof, A. van Blaaderen, and J.K.G. Dhont, Langmuir **10**, 3477 (1994).
[18] A. Imhof, A. van Blaaderen, G. Maret, J. Mellema, and J.K.G. Dhont, J. Chem. Phys. **100**, 2170 (1994).
[19] W.D. Dozier and P.M. Chaikin, J. Phys. (Paris) (France) **43**, 843 (1982).
[20] M.J. Stevens and M.O. Robbins, Phys. Rev. E **48**, 3778 (1993).
[21] F.W. Wiegel, *Fluid Flow Through Porous Macromolecular Systems*, Lecture Notes in Physics (Springer-Verlag, Berlin, 1980).
[22] B. Van der Vorst, D. van den Ende, and J. Mellema, J. Rheol. **39**, 1183 (1995).
[23] B.U. Felderhof and R.B. Jones, Faraday Discuss. Chem. Soc. **83** 1 (1987).
[24] R.R. De Rooij, A.A. Potanin, D. van den Ende, and J. Mellema, Colloid J. **56**, 549 (1994).
[25] T. Van Vliet, H. Luyten, and P. Walstra, in *Proceedings Symposium*, Norwich, 1990, edited by E. Dickinson (Royal Society of Chemistry, Cambridge, 1991), pp. 392–403.
[26] J.N. Shapiro, Phys. Rev. B **1**, 3982 (1970).
[27] C.G. De Kruif, E.M.F. van Iersel, A. Vrij, and W.B. Russel, J. Chem. Phys. **83**, 4717 (1985).
[28] H. Löwen, T. Palberg, and R. Simon, Phys. Rev. Lett. **70**, 1557 (1993).
[29] J.P. Hansen and I.R. McDonald, *Theory of Simple Liquids*

(Academic Press, New York, 1976), p. 361.
[30] J.W. Goodwin, J. Hearn, C.C. Ho, and R.H. Ottewill, Br. Polym. J. **5**, 347 (1973).
[31] J. Hearn, M.C. Wilkinson, and A.R. Goodall, Adv. Colloid Interface Sci. **14**, 173 (1981).
[32] L.B. Chen, B.J. Ackerson, and C.F. Zukoski, J. Rheol. **38**, 193 (1994).
[33] R. Buscall, Colloids Surf. A **83**, 33 (1994).
[34] M.K. Chow and C.F. Zukoski, J. Rheol. **39**, 33 (1994).